Universal Reset Characteristics of Unipolar and Bipolar Metal-Oxide RRAM

Daniele Ielmini, *Senior Member, IEEE*, Federico Nardi, *Student Member, IEEE*, and Carlo Cagli

***Abstract*—Set and reset characteristics are studied for unipolar and bipolar metal-oxide resistive-switching memory devices. We show a universal dependence of set-state resistance and reset current on the compliance current used during set, with negligible impact of metal-oxide composition and switching condition. An analytical Joule-heating model for universal reset is presented, predicting a weak dependence of reset temperature and voltage on diffusion and migration parameters in both unipolar- and bipolar-switching modes. Data for the reset voltage are shown for a wide range of unipolar and bipolar metal oxides, in support of our calculations.**

***Index Terms*—Memory modeling, nonvolatile memory, resistive-switching memory (RRAM).**

I. Introduction

RESISTIVE-switching memory (RRAM) devices based on reversible resistance change in metal oxides are considered a potential alternative to existing Flash technology for future nonvolatile memory downscaling [1]. In RRAM, the resistance is decreased in the *set* transition, consisting of the formation of a conductive filament (CF) by dielectric breakdown. The CF is subsequently disrupted in the *reset* transition, restoring a high-resistance state [2]. Two switching modes are generally observed: In *unipolar* switching, resistance change takes place irrespective of the pulse polarity [2], [3], while the polarity must be necessarily reversed for set and reset in *bipolar* switching [1]. Resistance switching studies have led to physical models for reset as a function of CF size, shape, and resistance [2], [4]–[6]. The reset operation is generally interpreted as a temperature-driven dissolution of the CF. However, for a deeper insight into the conduction and switching mechanisms on the nanometer scale, a comparative study of set/reset transitions for different active metal oxides is needed.

This work addresses set and reset characteristics for unipolar and bipolar RRAM with different metal oxides, providing evidence for a *universal* dependence of set-state resistance and reset current on current compliance I_C, which is the current during the set operation. Universal reset is explained by diffusion/migration processes responsible for CF rupture. It is shown that, due to the exponential dependence of CF dissolution rate on the local temperature, the reset voltage is generally in the range between 0.2 and 1 V, thus resulting in an almost universal relationship between compliance and reset current. Our analysis provides a strong physical basis for the modeling of conduction and switching in filamentary RRAM devices.

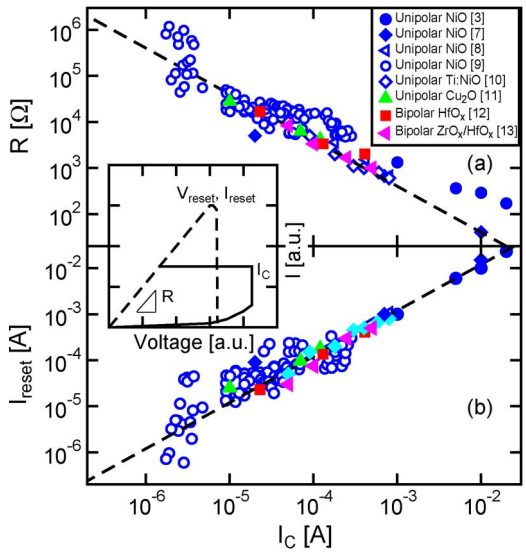

Fig. 1. Measured (a) set-state resistance R and (b) $I_{\rm reset}$ as a function of I_C. Data are shown for several unipolar and bipolar RRAM devices with different active materials, including NiO [3], [7]–[10], Cu_2O [11], HfO_x [12], and ZrO_x/HfO_x [13]. The inset shows the schematic I–V curves for (solid) unipolar set and (dashed) reset transitions, defining parameters I_C, $V_{\rm reset}$, $I_{\rm reset}$, and R.

II. Set/Reset Characteristics

Fig. 1(a) and (b) shows the measured set-state resistance R and reset current $I_{\rm reset}$, respectively, as a function of the current compliance I_C during set for various unipolar and bipolar RRAM devices [3], [7]–[13]. The inset shows the schematic I–V curves for unipolar set and reset transitions: The device is set under a compliance current I_C, resulting in a relatively low resistance R in the set state. In the following reset operation, the voltage is swept with no current limitation, resulting in a reset transition from low to high resistance at a reset voltage $V_{\rm reset}$ and a reset current $I_{\rm reset}$. In case the reset transition is not as abrupt as the one schematically shown in the inset, $V_{\rm reset}$ was taken as the voltage at which the resistance started to increase along the I–V curve. The figure includes data for different metal-oxide materials, such as unipolar-switching NiO [3], [7]–[10], unipolar-switching Cu_2O[11], bipolar-switching

Manuscript received March 28, 2011; revised May 18, 2011 and June 11, 2011; accepted June 21, 2011. Date of publication July 29, 2011; date of current version September 21, 2011. This work was supported in part by Intel under Project 55887 and in part by Fondazione Cariplo under Grant 2010-0500. The review of this paper was arranged by Editor R. Huang.

The authors are with the Dipartimento di Elettronica e Informazione and the Italian Universities Nanoelectronics Team (IU.NET), Politecnico di Milano, 20133 Milano, Italy (e-mail: ielmini@elet.polimi.it; nardi@elet.polimi.it; cagli@elet.polimi.it).

Color versions of one or more of the figures in this paper are available online at http://ieeexplore.ieee.org.

Digital Object Identifier 10.1109/TED.2011.2161088

HfO_x [12], and bipolar-switching ZrO_x/HfO_x [13]. All data were obtained through quasi-static (dc) voltage sweeps in a relatively long time range (about 1 s). The current during set was controlled according to different schemes, including the use of a current-compliance mode in current meters [3], [7], [10], [13] or the control of the gate voltage of a MOS transistor integrated in series with the RRAM cell in the so-called one-transistor/one-resistor (1T1R) structure [8], [9], [11], [12]. Irrespective of the method of current limitation, the data reported in the figure demonstrate that R and $I_{\rm reset}$ are tightly controlled by I_C, with no significant dependence on material composition, measurement scheme, or unipolar-/bipolar-switching mode.

It has been pointed out that the limitation of the current during the set operation is not always effective, due to possible current overshoots caused by the parasitic capacitance [8], [14], [15] or by the relatively slow response of the compliance system [7], [8]. In particular, it has been shown that current spikes may result in a saturation of R and $I_{\rm reset}$ for decreasing I_C below the current spike level [8]. However, the data in Fig. 1 indicate no sign of saturation in either R or $I_{\rm reset}$; thus, we may rule out the presence of significant parasitic current spikes affecting the CF formation and the final R value. This can be explained either by a relatively large I_C, largely exceeding the effects of possible current spikes, or by the minimization of the parasitic capacitance in 1T1R structures [8], [9], [11], [12]. On the other hand, parasitic current spikes may be responsible for the increased spread of R and $I_{\rm reset}$ for $I_C < 10\ \mu$A. In this low I_C range, in fact, even small capacitive overshoots may exceed the current compliance during set, thus affecting the final CF size. The statistical spread in small CFs may also be due to local shape/defect variability. In fact, the estimated size of a CF with several kΩ resistance is around few nanometers [16]; thus, even a small filament roughness or a fluctuation in the position/number of defects along the CF may cause relatively large fluctuations of resistance for a given I_C.

Despite the wide range of materials and switching polarity, all the data in Fig. 1 fall along the same trend [17]. In particular, R in Fig. 1(a) is inversely proportional to I_C according to the empirical law

$$R = \frac{V_0}{I_C} \tag{1}$$

where V_0 is about 0.4 V, while $I_{\rm reset}$ in Fig. 1(b) is proportional to I_C with a ratio $I_{\rm reset}/I_C$ of about 1.2. The dashed lines in the figure correspond to the two empirical laws of constant V_0 [Fig. 1(a)] and constant $I_{\rm reset}/I_C$ ratio [Fig. 1(b)]. From (1), one can estimate the reset voltage $V_{\rm reset}$ from the product $RI_{\rm reset} \approx V_0 I_{\rm reset}/I_C \approx 1.2 \times 0.4 \approx 0.5$ V. This indicates that the universal reset characteristic in the figure is due to an approximately constant $V_{\rm reset}$, irrespective of the unipolar-/bipolar-switching mode and of the oxide material used in the RRAM device.

III. Analytical Reset Model in Unipolar RRAM

To understand the universal reset characteristics of unipolar RRAM in Fig. 1, we considered the reset model based on the thermally activated CF dissolution [2], [6]. According to this model, during the application of a voltage sweep or pulse, the temperature within the CF increases, thus enhancing the probability for oxidation of the excess metallic elements (e.g., Ti in TiO_2 [18] or Ni in NiO [19]) which are responsible for the locally increased conductivity. The chemical reaction is believed to be mediated by metal or oxygen diffusion, possibly enhanced by defects such as vacancies or grain boundaries. Thus, the reset time $t_{{\rm reset},u}$ for unipolar CF rupture can be estimated as the time for radial diffusion through a distance ϕ equal to the CF diameter, namely [17]

$$t_{{\rm reset},u} = \frac{\phi^2}{D} = \frac{\phi^2}{D_0} e^{\frac{E_A}{kT}} \tag{2}$$

where T is the maximum temperature within the CF and the diffusion constant D is given by the Arrhenius law using a preexponential constant D_0 and the activation energy for diffusion E_A. The CF diameter ϕ increases for decreasing R [16], hence for increasing I_C based on the set characteristic in Fig. 1(a). From (2), the local temperature $T_{\rm reset}$ needed to trigger reset in the CF can be obtained as

$$T_{\rm reset} = \frac{E_A}{k \log\left(\frac{D_0 \tau}{\phi^2}\right)} \tag{3}$$

where τ is a typical timescale for the reset experiment.

Fig. 2(a) shows $T_{\rm reset}$ calculated by (3) as a function of D_0 and ϕ. These two parameters were changed in a broad range of six orders of magnitude (D_0 between 10^{-5} and 10 cm$^2 \cdot$ s^{-1}) and two orders of magnitude (ϕ between 1 and 100 nm), respectively. E_A was kept equal to 1.4 eV, close to the measured activation energy from reset and retention experiments in NiO [16], [20]. This value is also comparable to the calculated energy barrier for Ni vacancy diffusion in NiO [21], thus supporting the key role of diffusion as the limiting step in the reset process. A characteristic time $\tau = 10^{-2}$ s was used, corresponding to dc measurements. Due to the logarithmic dependence on D_0 and ϕ in (3), the calculated $T_{\rm reset}$ remains within a narrow range between 500 K and 2500 K, despite the large range assumed for D_0 and ϕ. From these results, $T_{\rm reset}$ may display only a weak dependence on host and CF materials, due to the logarithmic dependence on D_0 in Fig. 2(a). Similarly, different CF sizes may result in a relatively small change of $T_{\rm reset}$.

Note that the low-resistance state was assumed to be due to a *single* CF in both (2) and (3). In the case of multiple filaments being responsible for the low-resistance state in the memory, similar results would be obtained. In fact, assuming that R is due to N identical CFs instead of a single CF, the individual area of multiple CFs is N times smaller than the single-CF case. As a result, the reset temperature $T'_{\rm reset}$ for N parallel CFs becomes

$$T'_{\rm reset} = \frac{E_A}{k \log\left(\frac{N D_0 \tau}{\phi^2}\right)} \tag{4}$$

which is clearly smaller than $T_{\rm reset}$ in (3). However, due to the logarithmic dependence on N, the reset temperature remains almost unchanged with respect to the calculations in Fig. 2(a).

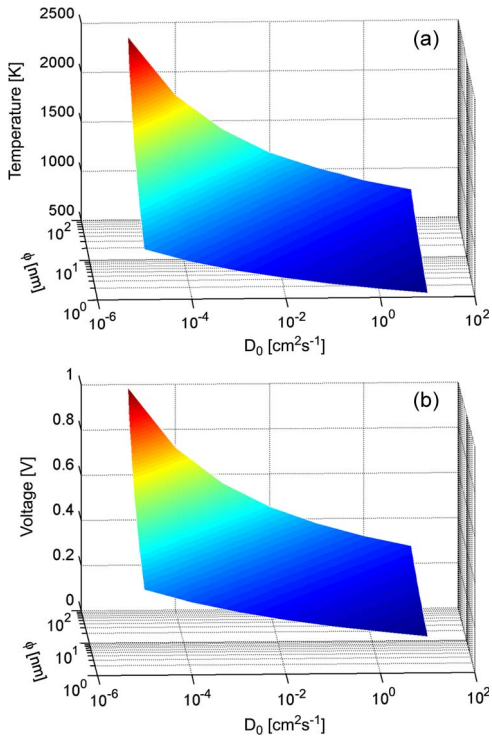

Fig. 2. Calculated (a) $T_{\rm reset}$ and (b) $V_{\rm reset}$ from (3) and (5), respectively, as a function of parameters D_0 and ϕ for unipolar-switching devices.

From the estimated $T_{\rm reset}$, we calculate the reset voltage $V_{\rm reset}$, namely, the voltage needed to raise the local CF temperature to the critical value $T_{\rm reset}$, from the steady-state solution of the Fourier equation for Joule heating, that is [2], [6]

$$V_{\rm reset} = \sqrt{\frac{R}{R_{\rm th}}(T_{\rm reset} - T_0)} \tag{5}$$

where $R_{\rm th}$ is the equivalent thermal resistance of the CF. For a metallic CF at $T_{\rm reset}$, the ratio between R and $R_{\rm th}$ can be given by the Wiedemann–Franz (WF) law for the ratio between thermal conductivity $k_{\rm th}$ and electrical conductivity σ, yielding [2]

$$\frac{R}{R_{\rm th}} = \frac{8k_{\rm th}}{\sigma} = 8LT_{\rm reset} \tag{6}$$

where $L = 2.48 \times 10^{-8}$ V$^2 \cdot$ K^{-2} is the Lorenz constant [17]. The factor 8 in (6) comes from the steady-state solution of the Fourier equation during reset in the CF and is due to the uniform Joule dissipation and the heat conduction toward the top and bottom heat sinks [2], [6]. Fig. 2(b) shows $V_{\rm reset}$ calculated by (5) as a function of D_0 and ϕ. Both parameters were chosen in the same range as in Fig. 2(a). Again, despite the large range of D_0 and ϕ, the reset voltage varies within a relatively small range from 0.2 to 1 V. This demonstrates that the unipolar reset model based on thermally activated CF dissolution can account for the weak dependence of $V_{\rm reset}$ on CF and host materials in the RRAM, consistently with data in Fig. 1.

Equation (6) assumes that Joule heating dissipated during reset mainly flows along the CF toward the top and bottom heat sinks [6]. On the other hand, assuming that $R_{\rm th}$ includes a nonnegligible contribution of heat loss through the metal-oxide region surrounding the CF, the ratio $R/R_{\rm th}$ may be larger than that in (6), thus leading to a larger $V_{\rm reset}$. Similarly, assuming that heat conduction includes a significant phonon contribution [2], larger values for $R/R_{\rm th}$ and, consequently, for $V_{\rm reset}$ may be obtained.

Equation (6) assumes that the CF has a metallic conduction characteristic, where both electrical and thermal conductions are controlled by electrons. This assumption is strictly valid only for relatively small R below 1 kΩ, since CFs with higher R typically display a semiconductorlike conduction [16]. However, it should be noted that the activation energy for conduction $E_{\rm AC}$, describing the semiconductorlike transport, is smaller than 0.1 eV for R below 100 kΩ, which represents the majority of data in Fig. 1. In addition, at high voltage close to the reset point, the carrier concentration in the semiconductorlike CF is highly enhanced, due to the following: 1) the field-induced barrier lowering, which decreases $E_{\rm AC}$ as in the Poole–Frenkel effect [6], and 2) the temperature-induced emission of carriers to the conduction/valence bands. These multiplication effects result in charge carriers providing the main contribution to thermal and electrical conductions close to the reset point, thus supporting the WF law for calculating the resistance ratio in (6).

Note also that the thermally activated reset model in (5) is experimentally supported by the evidence for the temperature dependence of reset parameters on the sample temperature T_0. For instance, it was shown that the reset power in unipolar NiO decreases for increasing T_0 as a result of the smaller temperature increase $\Delta T = T_{\rm reset} - T_0$ to reach the critical oxidation temperature [22]. Similar results were obtained for bipolar switching: For increasing T_0, $V_{\rm reset}$ was shown to decrease in bipolar HfO_2 [23], and the reset time at a given pulse voltage was shown to decrease in bipolar ZnO [24]. These evidences support the thermally activated CF dissolution model for both unipolar and bipolar switchings in RRAM operation.

IV. Analytical Reset Model in Bipolar RRAM

Although unipolar- and bipolar-switching RRAM devices share the same basic temperature-activated nature of the reset process, the radial diffusion model of the previous section strictly applies to unipolar switching only. In the case of bipolar switching, in fact, ion migration contributes to the dissolution process in addition to pure diffusion [1], [25]. This is schematically shown in Fig. 3, depicting the potential profiles for ion migration along the CF with and without an applied bias. Ions may consist of positive metallic ions, negative oxygen ions, or positive oxygen vacancies. Migration may be described by ion hopping among localized states, characterized by an effective energy barrier E_A, which we will assume equal to the activation energy for diffusion used in the previous section [25]–[28]. The application of a bias results in a barrier lowering for hopping; thus, the ion hopping rate $r_{\rm ion}$ can be given by [26]

$$r_{\rm ion} = r_0 e^{-\frac{E_A - q\alpha V}{kT}} \tag{7}$$

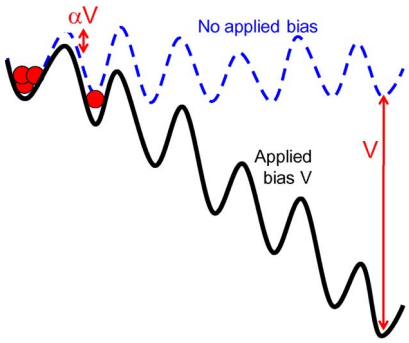

Fig. 3. Schematic illustration of the potential profile for ion hopping along the CF with and without an applied bias. Ions diffuse randomly when the applied voltage is zero. The barrier lowering αqV induces ion migration in the direction of the electrostatic force in the presence of an applied voltage V.

where r_0 is a preexponential factor and α is a coefficient controlling the barrier lowering effect. As shown in Fig. 3, αV gives the barrier lowering in the direction of the field for a positive ion [26]. Therefore, α may be approximated by $\Delta z/2L_{\rm CF}$, where Δz is the distance among ion hopping states and $L_{\rm CF}$ is the length of the filament. The latter may be assumed equal to the thickness of the oxide layer, in case of a CF with approximately uniform conductivity and cross section. Evidence for migration controlling set and reset in a bipolar-switching device comes from the fact that the polarity must be necessarily reversed for repeatable switching. Note that, although the electric field plays a key role in the ion migration owing to the barrier lowering effect in Fig. 3, the temperature dependence is nonetheless very important, given the Arrhenius model for ion migration in (7) [25]–[28]. Based on (7), the reset time $t_{{\rm reset},b}$ for bipolar switching can thus be obtained by a generalization of (2), where a voltage-dependent activation energy is used to describe ion migration in the direction of the electrostatic force, namely

$$t_{{\rm reset},b} = \frac{\phi^2}{D} = \frac{\phi^2}{D_0} e^{\frac{E_A - q\alpha V}{kT}} \tag{8}$$

where the voltage-induced barrier lowering has been included in the Arrhenius law. Using the Joule heating formula and $t_{{\rm reset},b} = \tau$, (8) yields a second-order equation in V, which can be solved to obtain a closed formula for the reset voltage $V_{\rm reset}$ (see the Appendix). Note that the approximation in (8) is physically consistent with the fact that, for decreasing V toward zero, the unipolar-switching formula of the previous section is recovered. In addition, the CF dissolution requires that its cross section is reduced to zero, thus justifying the dependence of $t_{{\rm reset},b}$ on the diameter ϕ (instead, e.g., of the CF length $L_{\rm CF}$) in (8). A slightly different model for CF dissolution in bipolar RRAM was proposed, assuming that the size reduction rate $d\phi/dt$ is proportional to the ion migration rate $r_{\rm ion}$ [28]. In that case, $t_{{\rm reset},b}$ would increase linearly with ϕ, differently from the quadratic dependence $t_{{\rm reset},b} \propto \phi^2$ in (8). However, due to the weak dependence of $T_{\rm reset}$ and $V_{\rm reset}$ on ϕ, this would only lead to minor changes in our conclusions (see the Appendix).

Fig. 4(a) shows the calculated $V_{\rm reset}$ for unipolar and bipolar switchings, obtained from (5) and (A5), respectively, as a function of ϕ. In the calculations, we used three different values of diffusivity, namely, $D_0 = 10^{-5}$, 10^{-2}, and 10 cm$^2 \cdot$ s^{-1}. A barrier lowering factor $\alpha = 0.3$ was used for bipolar switching [26], while no barrier lowering was assumed in unipolar switching ($\alpha = 0$). For a given D_0 and ϕ, the bipolar $V_{\rm reset}$ is lower than the unipolar case, due to the barrier lowering effect in (8). Results in the figure confirm that $V_{\rm reset}$ remains within a small range from 0.2 to 1 V even for bipolar RRAM, despite the large range of D_0 and ϕ. These results thus support a universal $V_{\rm reset}$ for both unipolar and bipolar switchings. In particular, the average $V_{\rm reset}$ of about 0.5 V in Fig. 1 can be obtained with $E_A = 1.4$ eV, $D_0 = 10^{-5}$ cm$^2 \cdot$ s^{-1}, and ϕ between 5 and 15 nm from Fig. 4(a).

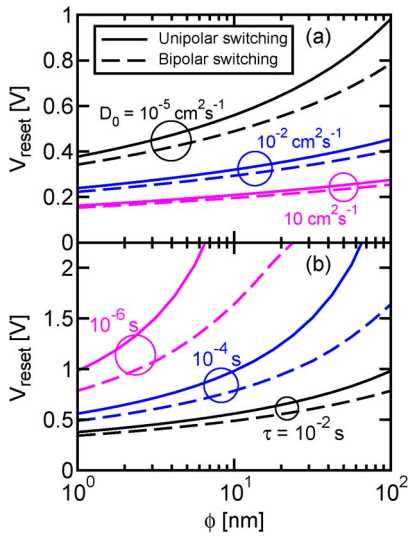

Fig. 4. Calculated $V_{\rm reset}$ as a function of ϕ for variable D_0 (a) and τ (b). $V_{\rm reset}$ is shown for (solid) unipolar-switching and (dashed) bipolar-switching RRAM, obtained from (5) and (A5), respectively.

It should be recalled that the relatively low $V_{\rm reset}$ in Figs. 1, 2, and 4(a) is obtained from a dc operation, namely, the application of slow voltage sweep to reset the cell, with a typical timescale from few milliseconds to 1 s. However, it is known that the reset voltage increases as the sweep rate is increased, thus decreasing the timescale of the experiment [20]. Equivalently, the time for reset decreases as the applied voltage increases [20]. Both these results are reproduced by the diffusion/migration model for reset. In fact, decreasing the timescale τ leads to an increase of the critical temperature, hence of the reset voltage, in (3). On the other hand, increasing the voltage (hence the temperature) results in a decrease of the reset time in both (2) and (8). Fig. 4(b) shows the calculated $V_{\rm reset}$ as a function of ϕ, for decreasing pulsewidth $\tau = 10^{-2}$, 10^{-4}, and 10^{-6} s, assuming $D_0 = 10^{-5}$ cm$^2 \cdot$ s^{-1}. Calculations were done for both unipolar ($\alpha = 0$) and bipolar switching ($\alpha = 0.3$). $V_{\rm reset}$ increases for decreasing τ, in agreement with previously reported results [20].

Note that, although Fig. 4 shows a comparable $V_{\rm reset}$ for unipolar and bipolar switchings, it does not imply that a given material will display both types of switching with very similar $V_{\rm reset}$. In fact, the "preference" of a certain material for unipolar or bipolar switching might depend on a number of parameters, including electrode materials and microstructure of

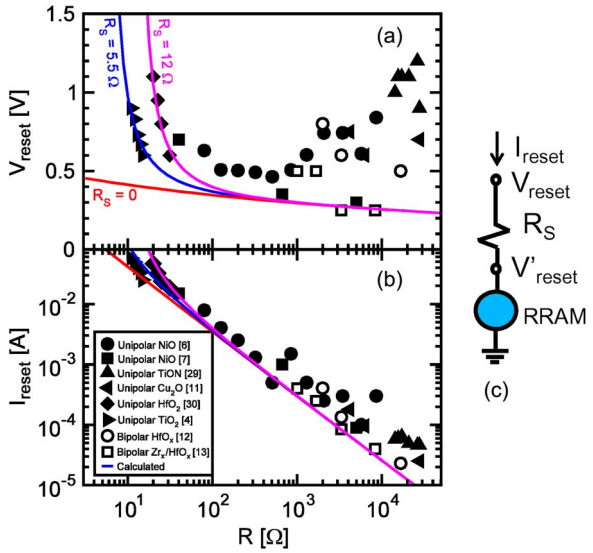

Fig. 5. Measured (a) $V_{\rm reset}$ and (b) $I_{\rm reset}$ as a function of R for several unipolar- and bipolar-switching RRAM, including NiO [6], [7], TiON [29], HfO_x [12], [30], Cu_2O [11], TiO_2 [4], and ZrO_x/HfO_x [13], and (c) schematic for the series resistance effect contributing to the increase of $V_{\rm reset}$ at low R. Calculations are shown in (a) and (b) according to (9) with/without correction by the series resistance effect.

the insulating oxide. These aspects will be further discussed in Section VI.

V. Reset Voltage Analysis

To validate the calculation results in Figs. 2 and 4, indicating a universal $V_{\rm reset}$, Fig. 5(a) and (b) shows the measured $V_{\rm reset}$ and $I_{\rm reset}$, respectively, as a function of R for several metal oxides, including NiO [6], [7], TiON [29], HfO_x [12], [30], Cu_2O [11], TiO_2 [4], and ZrO_x/HfO_x [13]. Data for both unipolar [4], [6], [7], [11], [29], [30] and bipolar switching [12], [13] are compared in the figures. Most $V_{\rm reset}$ data are limited between 0.5 and 1 V, consistently with calculations in Figs. 2 and 3, while $I_{\rm reset}$ decreases according to the phenomenological behavior $I_{\rm reset} \approx V_{\rm reset}/R \propto R^{-1}$, in agreement with the universal reset characteristic in Fig. 1. The unipolar $V_{\rm reset}$ increases for increasing R, which was explained as a different increase of R and $R_{\rm th}$ for small filaments [6]. In fact, $R_{\rm th}$ may become increasingly dominated by heat loss through the surrounding metal oxide for decreasing ϕ, thus resulting in a decreased heating efficiency according to (3). An increasing $V_{\rm reset}$ might also be due to a nonuniform CF with relatively high R obtained by partial reset [6]. Partial reset may, in fact, induce a depleted gap with higher resistivity along the CF, thus leading to a localization of the electric field in the gap and a consequent inhibition of reset in the undepleted region. On the other hand, $V_{\rm reset}$ increases for decreasing R, as shown by unipolar RRAM for R below 100 Ω. This might be partially due to a size-dependent reset effect, where a CF with a relatively large ϕ requires a higher $T_{\rm reset}$ and $V_{\rm reset}$ according to Figs. 2 and 3.

The size-dependent reset, however, cannot fully explain the steep rise of $V_{\rm reset}$ for decreasing R below 40 Ω in Fig. 5(a) [4], [7], [30]. To account for the strong increase of $V_{\rm reset}$ in the figure, we consider the possible effect of a series resistance R_S in the RRAM device, as shown in Fig. 5(c). Due to the presence of the series resistance, the "apparent" reset voltage $V_{\rm reset}$ is, in fact, given by

$$V_{\rm reset} = V'_{\rm reset} + R_S I_{\rm reset} = V'_{\rm reset}\left(1 + \frac{R_S}{R'}\right) \qquad (9)$$

where $V'_{\rm reset}$ and R' are, respectively, the "true" reset voltage and resistance of the RRAM device. This additional voltage drop largely increases for $R' \ll R_S$, thus contributing to the steep rise of $V_{\rm reset}$ at small R in Fig. 5(a). Calculations according to (9) are also shown in Fig. 5(a) and (b), assuming $D_0 = 10^{-5}$ cm$^2 \cdot$ s^{-1}, $E_A = 1.4$ eV, and a CF size obtained from $R = \rho t_{\rm ox}/A$, with a metallic resistivity $\rho = 10$ $\mu\Omega \cdot$ cm and $t_{\rm ox} = 25$ nm. For instance, $R_S = 5.5$ and 12 Ω can account for the observed $V_{\rm reset}$ in unipolar TiO_2 [4] and HfO_2 [30], respectively. The series resistance effect might also explain the decrease of $V_{\rm reset}$ for increasing R for bipolar RRAM devices, assuming a relatively large R_S around 0.5 kΩ [12], [13]. With a proper selection of D_0 and R_S, the reset model may account for all data in Fig. 5, while the $V_{\rm reset}$ increase at high R may require a slightly more sophisticated description for the CF nonuniformity and thermal resistance, as discussed earlier.

VI. Discussion

The weak dependence of $V_{\rm reset}$ on material, initial R, and switching mode, which is fully explained by our analysis in Figs. 2 and 4, can account for the universal reset of unipolar and bipolar RRAM in Fig. 1(b). While the reset model applies to all metal-oxide RRAM, it may not account for resistance switching effects observed in RRAM devices based on carbon [31] and SiO_2 [32]. These devices, in fact, usually display larger $V_{\rm reset}$, which might be due to series resistance effects as discussed in the previous section or to a completely different reset mechanism.

Although the reset model can predict the reset temperature and voltage for a given pulsewidth τ and a given set of microscopic parameters (E_A, ϕ, D_0, α), it is unable to explain and predict whether a unipolar or a bipolar switching should be expected in a given material. A coexistence of unipolar- and bipolar-switching modes has been demonstrated in some materials, including TiO_x [33], [34], NiO [35], and ZnO [36]. On the other hand, other materials are known to display only unipolar or bipolar switching. The reason for the preference of a material system for a specific switching mode might depend on a number of factors. It has been highlighted that ion migration plays a key role in bipolar switching. Assuming that set and reset are performed under positive and negative voltages, respectively, in a bipolar RRAM device, carrying out a unipolar reset under positive voltage might be difficult, due to the competition between set and reset. In fact, on the one hand, the CF is reinforced due to ion migration, while on the other hand, thermally activated diffusion according to the unipolar model in Section III might induce CF dissolution. The set/reset competition may explain the absence of unipolar reset in some

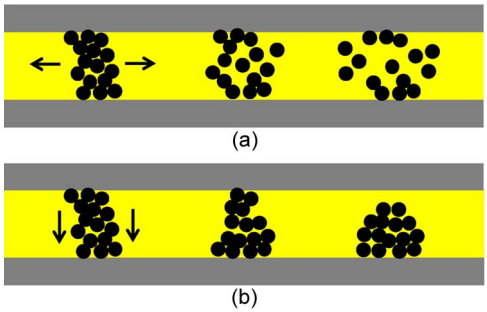

Fig. 6. Schematic snapshots of a reset process in (a) unipolar and (b) bipolar RRAM. Snapshots are shown for increasing time from left to right. Reset is due to thermally activated radial diffusion in unipolar RRAM, resulting in a self-accelerated dissolution of the CF (a). Temperature- and voltage-induced vertical migration of ions is instead responsible for bipolar reset (b).

bipolar RRAM: The reset sweep, in fact, increasingly reinforces the CF, leading to an irreversible hard breakdown. Alternatively, unipolar reset in bipolar metal oxides may result in a destructive event due to the radial diffusion of conductive elements far from the CF, thus making the restoration of a continuous filament impossible.

Other metal oxides might not show any preference to bipolar switching, and this could be explained by a difficult or poor ionization of CF metallic species, which are thus immune from voltage-driven migration effects. In this case, the barrier lowering is ineffective, while the concentration gradient may be the strongest driving force for dissolution, thus inducing a CF reset by radial diffusion, as shown in Fig. 6(a).

Another key difference in the reset behavior of unipolar- and bipolar-switching devices is the abruptness of the transition in the I–V curves. In fact, unipolar reset typically displays an abrupt increase of resistance [2]–[6]. This has been attributed to a self-accelerated thermal dynamics of CF dissolution: As the CF cross section decreases due to oxidation, field and current localization along the CF increases, thus enhancing Joule heating and the consequent acceleration of diffusion and chemical reaction [22], [34]. On the other hand, bipolar reset shows a gradual transition from low to high resistance during reset [12], [13], [34], [37]. The gradual transition suggests a self-limiting reset dynamics, where the reduction of conductivity in the CF inhibits further dissolution. The reset models proposed in this work can be used to calculate the temperature and the voltage for the onset of reset for unipolar and bipolar switchings; however, they cannot provide details about the dissolution dynamics in the CF after the onset of reset.

Finally, it is known that bipolar switching typically displays a longer cycling endurance as compared to unipolar switching. This may be due to the different reset mechanisms assumed in our reset models and qualitatively described in Fig. 6. Unipolar reset [Fig. 6(a)] consists of a radial diffusion of conductive elements/defects from the CF, thus causing a loss of conductivity. As a result, the conductive elements might not be available for CF rebuilt after repetitive unipolar reset, leading to endurance limitations. In addition, the temperatures and voltages for unipolar reset are typically larger, as also apparent from the calculations in Fig. 4, and this may result in an accelerated electromigration of metallic atoms from the electrodes, thus affecting endurance. On the other hand, bipolar reset [Fig. 6(b)] mostly occurs by voltage-/temperature-induced ion migration along the filament, thus resulting in no loss of the conductive species from the CF site. The repeatable ion migration according to the alternate biasing of the CF and the relatively low set/reset temperatures might explain the generally high endurance of the bipolar RRAM devices.

VII. Conclusion

Set and reset processes in metal-oxide RRAM are shown to obey universal characteristics, where I_C controls set/reset with negligible dependence on material and switching mode. The universal reset is explained through analytical models describing reset by thermally activated diffusion in unipolar RRAM or by voltage-/temperature-induced ion migration in bipolar RRAM. In both cases, a universal reset voltage is obtained, which remarkably agrees with experimental results for a wide range of metal-oxide RRAM. The universal $V_{\rm reset}$ is explained by the logarithmic dependence of diffusion and migration processes on CF parameters, such as diffusivity/migration prefactors and CF size.

Appendix

Using the Joule heating formula [6]

$$T = T_0 + \frac{R_{\rm th}}{R} V^2 \tag{A1}$$

and computing the logarithm in the left- and right-hand sides of (8), one obtains the reset condition

$$\log \frac{\tau D_0}{\phi^2} = \frac{E_A - q\alpha V_{\rm reset}}{k\left(T_0 + \frac{R_{\rm th}}{R} V_{\rm reset}^2\right)} \tag{A2}$$

which can be rearranged into

$$\frac{R_{\rm th}}{RT_0} V_{\rm reset}^2 + \frac{\eta q \alpha}{E_A} V_{\rm reset} + 1 - \eta = 0 \tag{A3}$$

where η is given by

$$\eta = \frac{E_A}{kT_0 \log \frac{D_0 \tau}{\phi^2}}. \tag{A4}$$

Solution of (A3) yields

$$V_{\rm reset} = \frac{\alpha \eta q R T_0}{2E_A R_{\rm th}} \left(\sqrt{1 + \frac{8R_{\rm th}E_A^2}{\alpha^2 \eta^2 q^2 R T_0}} - 1 \right) \tag{A5}$$

where (6) can be used to estimate $R/R_{\rm th}$. Equation (A5) can be used to calculate the bipolar reset voltage as a function of CF size ϕ for increasing D_0 [Fig. 4(a)] and τ [Fig. 4(b)]. Note that $V_{\rm reset}$ is a weak function of D_0 and ϕ through the factor η, similarly to (3) and (5) for unipolar reset.

A slightly different bipolar reset model involves the migration rate in (7) and a linear velocity for filament size reduction during reset [28]. According to this model, the bipolar reset time is given by

$$t_{{\rm reset},b} = \frac{\phi}{2r} = \frac{\phi}{2r_0} e^{\frac{E_A - q\alpha V}{kT}}. \tag{A6}$$

This leads to the same equation (A5) for $V_{\rm reset}$, provided that η is replaced by a constant η' given by

$$\eta' = \frac{E_A}{kT_0 \log \frac{2r_0\tau}{\phi}} \tag{A7}$$

which is very similar to (A4). Using (A6), instead of (8) for bipolar reset, our conclusions about the weak dependence of $V_{\rm reset}$ on material properties [D_0 in (8) or r_0 in (A6)] and CF size (ϕ) at the basis of the universal reset behavior remain unaffected.

REFERENCES

[1] R. Waser and M. Aono, "Nanoionics-based resistive switching memories," *Nat. Mater.*, vol. 6, no. 11, pp. 833–840, Nov. 2007.

[2] U. Russo, D. Ielmini, C. Cagli, and A. L. Lacaita, "Filament conduction and reset mechanism in NiO-based resistive-switching memory (RRAM) devices," *IEEE Trans. Electron Devices*, vol. 56, no. 2, pp. 186–192, Feb. 2009.

[3] S. Seo, M. J. Lee, D. H. Seo, E. J. Jeoung, D.-S. Suh, Y. S. Joung, I. K. Yoo, I. R. Hwang, S. H. Kim, I. S. Byun, J.-S. Kim, J. S. Choi, and B. H. Park, "Reproducible resistance switching in polycrystalline NiO films," *Appl. Phys. Lett.*, vol. 85, no. 23, pp. 5655–5657, Dec. 2004.

[4] K. M. Kim and C. S. Hwang, "The conical shape filament growth model in unipolar resistance switching of TiO_2 thin film," *Appl. Phys. Lett.*, vol. 94, no. 12, p. 122 109, Mar. 2009.

[5] K. M. Kim, M. H. Lee, G. H. Kim, S. J. Song, J. Y. Seok, J. H. Yoon, and C. S. Hwang, "Understanding structure-property relationship of resistive switching oxide thin films using a conical filament model," *Appl. Phys. Lett.*, vol. 97, no. 16, p. 162912, Oct. 2010.

[6] D. Ielmini, C. Cagli, and F. Nardi, "Physical models of size-dependent nanofilament formation and rupture in NiO resistive switching memories," *Nanotechnology*, vol. 22, no. 25, p. 254022, Jun. 2011.

[7] L. Goux, J. G. Lisoni, X. P. Wang, M. Jurczak, and D. J. Wouters, "Optimized Ni oxidation in 80-nm contact holes for integration of forming-free and low-power Ni/NiO/Ni memory cells," *IEEE Trans. Electron Devices*, vol. 56, no. 10, pp. 2363–2368, Oct. 2009.

[8] K. Kinoshita, K. Tsunoda, Y. Sato, H. Noshiro, S. Yagaki, M. Aoki, and Y. Sugiyama, "Reduction in the reset current in a resistive random access memory consisting of NiO_x brought about by reducing a parasitic capacitance," *Appl. Phys. Lett.*, vol. 93, no. 3, p. 033506, Jul. 2008.

[9] F. Nardi, D. Ielmini, C. Cagli, S. Spiga, M. Fanciulli, L. Goux, and D. J. Wouters, "Sub-10 μA reset in NiO-based resistive switching memory (RRAM) cells," in *Proc. IEEE IMW*, 2010, p. 66.

[10] K. Tsunoda, K. Kinoshita, H. Noshiro, Y. Yamazaki, T. Iizuka, Y. Ito, A. Takahashi, A. Okano, Y. Sato, T. Fukano, M. Aoki, and Y. Sugiyama, "Low power and high speed switching of Ti-doped NiO ReRAM under the unipolar voltage source of less than 3 V," in *IEDM Tech. Dig.*, 2007, pp. 767–770.

[11] T.-N. Fang, S. Kaza, S. Haddad, A. Chen, Y.-C. Wu, Z. Lan, S. Avanzino, D. Liao, C. Gopalan, S. Choi, S. Mahdavi, M. Buynoski, Y. Lin, C. Marrian, C. Bill, M. VanBuskirk, and M. Taguchi, "Erase mechanism for copper oxide resistive switching memory cells with nickel electrode," in *IEDM Tech. Dig.*, 2006, pp. 789–792.

[12] H. Y. Lee, P. S. Chen, T. Y. Wu, Y. S. Chen, C. C. Wang, P. J. Tzeng, C. H. Lin, F. Chen, C. H. Lien, and M.-J. Tsai, "Low power and high speed bipolar switching with a thin reactive Ti buffer layer in robust HfO_2 based RRAM," in *IEDM Tech. Dig.*, 2008, pp. 297–300.

[13] J. Lee, J. Shin, D. Lee, W. Lee, S. Jung, M. Jo, J. Park, K. P. Biju, S. Kim, S. Park, and H. Hwang, "Diode-less nano-scale ZrO_x/HfO_x RRAM device with excellent switching uniformity and reliability for high-density cross-point memory applications," in *IEDM Tech. Dig.*, 2010, pp. 452–455.

[14] D. Ielmini, D. Mantegazza, A. L. Lacaita, A. Pirovano, and F. Pellizzer, "Parasitic reset in the programming transient of phase change memories," *IEEE Electron Device Lett.*, vol. 26, no. 11, pp. 799–801, Nov. 2005.

[15] D. Ielmini, C. Cagli, and F. Nardi, "Resistance transition in metal oxides induced by electronic threshold switching," *Appl. Phys. Lett.*, vol. 94, no. 6, p. 063511, Feb. 2009.

[16] D. Ielmini, F. Nardi, C. Cagli, and A. L. Lacaita, "Size-dependent retention time in NiO-based resistive switching memories," *IEEE Electron Device Lett.*, vol. 31, no. 4, pp. 353–355, Apr. 2010.

[17] D. Ielmini, F. Nardi, and C. Cagli, "Universal switching and noise characteristics of nanofilaments in metal-oxide RRAMs," presented at the IEEE Semiconductor Interface Specialist Conf. (SISC), San Diego, CA, Dec. 2–4, 2010.

[18] D.-H. Kwon, K. M. Kim, J. H. Jang, J. M. Jeon, M. H. Lee, G. H. Kim, X.-S. Li, G.-S. Park, B. Lee, S. Han, M. Kim, and C. S. Hwang, "Atomic structure of conducting nanofilaments in TiO_2 resistive switching memory," *Nat. Nanotechnol.*, vol. 5, no. 2, pp. 148–153, Feb. 2010.

[19] G.-S. Park, X.-S. Li, D.-C. Kim, R.-J. Jung, M.-J. Lee, and S. Seo, "Observation of electric-field induced Ni filament channels in polycrystalline NiO_x film," *Appl. Phys. Lett.*, vol. 91, no. 22, p. 222103, Nov. 2007.

[20] C. Cagli, F. Nardi, and D. Ielmini, "Modeling of set/reset operations in NiO-based resistive-switching memory (RRAM) devices," *IEEE Trans. Electron Devices*, vol. 56, no. 8, pp. 1712–1720, Aug. 2009.

[21] T. Karakasidis and M. Meyer, "Grain-boundary diffusion of cation vacancies in nickel oxide: A molecular-dynamics study," *Phys. Rev. B, Condens. Matter*, vol. 55, no. 20, pp. 13 853–13 864, May 1997.

[22] U. Russo, D. Ielmini, C. Cagli, A. L. Lacaita, S. Spiga, C. Wiemer, M. Perego, and M. Fanciulli, "Conductive-filament switching analysis and self-accelerated thermal dissolution model for reset in NiO-based RRAM," in *IEDM Tech. Dig.*, 2007, pp. 775–778.

[23] Z. Fang, H. Y. Yu, W. J. Liu, Z. R. Wang, X. A. Tran, B. Gao, and J. F. Kang, "Temperature instability of resistive switching on HfO_2-based RRAM devices," *IEEE Electron Device Lett.*, vol. 31, no. 5, pp. 476–478, May 2010.

[24] B. Gao, B. Sun, H. Zhang, L. Liu, X. Liu, R. Han, J. Kang, and B. Yu, "Unified physical model of bipolar oxide-based resistive switching memory," *IEEE Electron Device Lett.*, vol. 30, no. 12, pp. 1326–1328, Dec. 2009.

[25] S. Yu and H.-S. P. Wong, "A phenomenological model for the reset mechanism of metal oxide RRAM," *IEEE Electron Device Lett.*, vol. 31, no. 12, pp. 1455–1457, Dec. 2010.

[26] U. Russo, D. Kalamanathan, D. Ielmini, A. L. Lacaita, and M. Kozicki, "Study of multilevel programming in programmable metallization cell (PMC) memory," *IEEE Trans. Electron Devices*, vol. 56, no. 5, pp. 1040–1047, May 2009.

[27] R. Meyer, L. Schloss, J. Brewer, R. Lambertson, W. Kinney, J. Sanchez, and D. Rinerson, "Oxide dual-layer memory element for scalable non-volatile cross-point memory technology," in *Proc. NVMTS*, 2008, pp. 1–5.

[28] D. Kamalanathan, U. Russo, D. Ielmini, and M. N. Kozicki, "Voltage-driven ON-OFF transition and tradeoff with program and erase current in programmable metallization cell (PMC) memory," *IEEE Electron Device Lett.*, vol. 30, no. 5, pp. 553–555, May 2009.

[29] Y. H. Tseng, C.-E. Huang, C.-H. Kuo, Y.-D. Chih, and C. J. Lin, "High density and ultra small cell size of Contact ReRAM (CR-RAM) in 90 nm CMOS logic technology and circuits," in *IEDM Tech. Dig.*, 2009, pp. 109–112.

[30] Y.-M. Kim and J.-S. Lee, "Reproducible resistance switching characteristics of hafnium oxide-based nonvolatile memory devices," *J. Appl. Phys.*, vol. 104, no. 11, p. 114115, Dec. 2008.

[31] F. Kreupl, R. Bruchhaus, P. Majewski, J. B. Philipp, R. Symanczyk, T. Happ, C. Arndt, M. Vogt, R. Zimmermann, A. Buerke, A. P. Graham, and M. Kund, "Carbon-based resistive memory," in *IEDM Tech. Dig.*, 2008, pp. 521–524.

[32] K.-P. Chang, H.-T. Lue, K.-Y. Hsieh, and C.-Y. Lu, "A SiO_2 nano-thermal unipolar 0T-1R ReRAM device with built-in diode isolation," in *Proc. Ext. Abs. Int. Conf. Solid State Devices Mater.*, 2010, p. 1100.

[33] D. S. Jeong, H. Schroeder, and R. Waser, "Coexistence of bipolar and unipolar resistive switching behaviors in a $Pt/TiO_2/Pt$ stack," *Electrochem. Solid-State Lett.*, vol. 10, no. 8, pp. G51–G53, 2007.

[34] W. Wang, S. Fujita, and S. S. Wong, "RESET mechanism of TiO_x resistance-change memory device," *IEEE Electron Device Lett.*, vol. 30, no. 7, pp. 733–735, Jul. 2009.

[35] L. Goux, J. G. Lisoni, M. Jurczak, D. J. Wouters, L. Courtade, and C. Muller, "Coexistence of the bipolar and unipolar resistive-switching modes in NiO cells made by thermal oxidation of Ni layers," *J. Appl. Phys.*, vol. 107, no. 2, p. 024512, Jan. 2010.

[36] S. Lee, H. Kim, J. Park, and K. Yong, "Coexistence of unipolar and bipolar resistive switching characteristics in ZnO thin films," *J. Appl. Phys.*, vol. 108, no. 7, p. 076101, Oct. 2010.

[37] J. Park, S. Jung, J. Lee, W. Lee, S. Kim, J. Shin, and H. Hwang, "Resistive switching characteristics of ultra-thin TiO_x," *Microelectron. Eng.*, vol. 88, no. 7, pp. 1136–1139, Jul. 2011.

Daniele Ielmini (M'04–SM'09) was born in 1970. He received the Laurea (*cum laude*) and Ph.D. degrees in nuclear engineering from the Politecnico di Milano, Milano, Italy, in 1995 and 1999, respectively.

In 1999, he joined the Dipartimento di Elettronica e Informazione, Politecnico di Milano, where he became an Assistant Professor in 2002 and Associate Professor in 2010. He held visiting positions at Intel Corporation, Santa Clara, CA, and Stanford University, Stanford, CA, in 2006. His most recent research interests include the modeling and the characterization of emerging nonvolatile memories, such as phase change memory and resistive switching memory (RRAM). He has authored/coauthored two book chapters and more than 160 papers published in international journals and presented at international conferences and is the holder of three patents.

Dr. Ielmini has served in several technical subcommittees of international conferences such as IEEE International Reliability Physics Symposium (2006–2008), Semiconductor Interface Specialist Conference (2008–2010), International Electron Device Meeting (2008–2009), and Insulating Films on Semiconductors (2011).

Federico Nardi (S'10) was born in Milano, Italy, in 1984. He received the B.S. and M.S. degrees in electronic engineering from the Politecnico di Milano, Milano, in 2006 and 2008, respectively.

For his first-level graduation thesis, he worked on electrical characterization of organic nonvolatile memories, and for his second-level graduation thesis, he studied resistive-switching effects in oxide-based memories (RRAMs). During 2010, he was a visiting Ph.D. student at the Institut Matériaux Microélectronique Nanosciences de Provence, Marseille, France. He is currently working with the Dipartimento di Elettronica ed Informazione, Politecnico di Milano, as Ph.D. student in information technology engineering and as a Teaching Assistant. He is also with the Italian Universities Nanoelectronics Team, Politecnico di Milano. His research interests include the characterization and modeling of electrical and physical properties in new emerging nonvolatile memories.

Carlo Cagli was born in Naples, Italy, in 1984. He received the Ph.D. degree from the Politecnico di Milano, Milano, Italy, in 2011.

During his thesis, he focused on electrical characterization and physics-based modeling of NiO-based RRAM devices. He is currently holding a Postdoc position with CEA-Minatec, Grenoble, France, where he is continuing his researches on oxide-based emerging memories.